Electronic Supplementary Information

Supplementary Experimental

DNA preparation

Synthetic DNA with a length of 148 bp was bought dry, desalted from Microsynth AG (Template MS, Balgach, CH). Sequences are provided in Table S1. Before use, the DNA with length 148 nt was diluted to 10 nM in deionized water and amplified for 11 cycles with qPCR (Roche LightCycler 480 II) according to the following parameters: 20 µL reactions in total contain 10 µL master mix (KAPA SYBR FAST for LightCycler 480), 1 µL forward and reverse primer each (Primer 0F/0R, 10 µM Microsynth AG), 3 µL deionized water (MicroPure UV, Thermo Scientific) and 5 µL DNA template. The cycling parameters were 15 s denaturation at 95°C, 15 s annealing at 56°C and 10 s extension at 72°C with a 5 min pre-incubation in the beginning. Eight reaction wells (160µL) were combined and purified in a silica column (DNA Clean & Concentrator-5, Zymo Research) according to the manufacturer's protocol. Briefly, 500 µL binding buffer was added and the mixture was applied to a column which was washed twice with 200 µL wash buffer. Purified DNA was eluted in 20 µL deionized water. The resulting solution was diluted to 30 ng μL^{-1}.

Deoxyribonucleic acid sodium salt from salmon testes (50 mg, Sigma) was dissolved in 5 mL deionized water in a 15 mL Falcon tube under rigorous shaking for 1 h at room temperature resulting in a viscous solution. For PXRD measurements, the DNA was sheared with an ultrasonic processor (UP50H, Hielscher) for 30 min with full amplitude and 90% time-averaged cycles. To prevent overheating, shearing was conducted in an ice bath. The sheared solution was centrifuged (3-30KS, Sigma) at 5000 rpm for 10 minutes and decanted to counteract solids contamination. Desalting was performed with dialysis for 2 days (Pur-A-LyzerMega 12000, Sigma-Aldrich) to exchange Na^+ ions. The resulting salmon testes DNA stock solutions contained approximately 5 g L^{-1}.

Table S1: DNA used for qPCR measurements.

Label	Sequence
Template MS	ACA CGA CGC TCT TCC GAT CTG ACT CTC ATC TAC TAG ATA GAT CTC CAC CTC GCA GT CTC GTC TTC AAC GGT GCT CAC GCG ATA TAG TTA GCT CGC GAC TAC CAT AGC GCT AC ATA GAA GTC AGC AAG AGA TCG GAA GAG CAC ACG TCT
Primer 0F (MS)	ACA CGA CGC TCT TCC GAT CT
Primer 0R (MS)	AGA CGT GTG CTC TTC CGA TCT
Primer OnKeta-spDL-F3	CCC GCA CAT TTG TAA ATG C
Primer OnKeta-spDL-R3	TGA TGT ATG AGG GGT TAA AAT AAG

Accelerated aging experiments

DNA decay experiments were conducted in 2 mL Eppendorf tubes: 1 µL of DNA (approximately 30 ng) was precipitated by first adding 5 µL of a mixture of potassium di-hydrogenphosphate (KH_2PO_4, 0.1 mM, ABCR) and di-potassium hydrogenphosphate tri-hydrate ($K_2HPO_4 \cdot 3\ H_2O$, 0.1 mM, Sigma-Aldrich). We will refer to this mixture as KP solution. Next, 5 µL of calcium chloride solution ($CaCl_2$ (0.1 mM), Sigma-Aldrich) was added, to precipitate 18 wt% DNA in calcium phosphate (CaP). The drying process included either 30 min centrifugation at 45°C under vacuum (<20 mbar, Concentrator plus vacuum centrifuge, Eppendorf) or 5 days in a refrigerator and 4°C with humidity control at 65% RH. Humidity was set with an open solution of saturated sodium bromide (NaBr) in deionized water in a PE storage container. To accelerate the aging process, tubes were stored in a desiccator with saturated NaBr solution to sustain 50% RH at 70°C for 0 to 6 days. The degradation extent was determined by measuring the remaining DNA amplifiable in a qPCR experiment and comparison to equal but not heat-treated samples. For this purpose, 100 µL of EDTA solution (1 mM, Fisher bioreagents) was added to redisperse DNA and consequently diluted 1:20 in deionized water prior to qPCR.

Powder X-Ray diffraction (PXRD)

Similar to accelerated aging sample preparation, DNA was precipitated in the presence of a phosphate and calcium source. 400 µL of sheared salmon stock solution (1.75 mg) was precipitated with 300 µL of KP solution and 300 µL of $CaCl_2$ solution (18 wt% loading of DNA) on a watch glass. Control samples contained no DNA. The drying step was either room temperature for 5 days, 30 min centrifugation at 45°C under vacuum (<20 mbar, Concentrator plus vacuum centrifuge, Eppendorf), 5 days in a refrigerator and 4°C with humidity control at 65% RH or without. PXRD was recorded using a PANalytical X'Pert PRO-MPD diffractometer with a Cu-Kα

radiation source (λ=1.5406 Å). The measurement range was 10° to 70° and 0.033° step size. The background was manually subtracted and the intensity normalized to the potassium chloride reflection on the (200) plane since it showed a comparable intensity for all measurements. Patterns were analyzed with the PANalytical X'Pert HighScore Plus (PW3212) software. Miller indices were assigned by pattern matching with the software database. Primary references for sylvite[1] and brushite[2] are indicated.

The quantitative analysis of the phase composition of aged DNA in calcium phosphate was performed on independent samples that were placed in an oven after synthesis/drying and for the diffractograms displayed in Figure 2 in the main text. Samples were carefully ground to a fine powder and loosely distributed over a zero diffraction plate. No background correction or normalization was conducted. The Rietveld analysis for phase composition analysis of the and quickly dried samples in Figure 2 was performed using TOPAS 7.[3] For the latter, the two peaks between 25 and 27°θ were excluded. The structures of monoclinic brushite ($Ca[PO_3(OH)]\cdot 2\ H_2O$), triclinic monetite ($CaHPO_4$) and cubic sylvite (KCl) were matched to all collected diffraction datasets. Brushite was fully restructured into monetite at the beginning of the heat treatment. Hence, models composed of brushite and KCl were fitted to data at 0h oven time and models for monetite and KCl were fitted to data at 10 h, 24 h and 48 h oven time, respectively. Slowly dried samples (Fig. 2) were fitted using Pawley refinement. The profile of the Bragg reflections was described with a Pseudo-Voight function. The preferential orientation of the brushite phase needed to be corrected by means of a March-Dollase macro, defined in (010) direction.

Scanning electron microscopy (SEM) and energy-dispersive X-ray spectroscopy (EDX)

DNA precipitation and drying was performed exactly as for qPCR (synthetic DNA) and PXRD (genomic DNA). Several mg of sample were deposited on an adhesive stub. For synthetic DNA samples, the eppendorf tube of a dried sample was cut at the bottom and placed on the adhesive stub. A conductive layer of platinum was sputtered on to prevent charging of the sample during measurements with a sputter coater(Agar, 30 s, 35 mA). SEM micrographs and EDX measurements (EDAX Team software) were recorded with a FEI, NovaNanoSEM 450 instrument using a beam voltage of 30.0 kV.

Diffuse reflectance infrared spectrometry (DRIFTS)

Samples were prepared similarly as for PXRD. 300 µL of salmon stock solution (1.5 mg) was precipitated with 208 µL of KP solution and 208 µL of $CaCl_2$ solution (18 wt% loading of DNA) on an watchglass and dried under vacuum or in the refrigerator. Control samples contained no DNA or no CaP. The dried sample was combined with 30 mg of KBr and 2.5±0.1 mg of potassium

ferricyanide ($K_3[Fe(CN)_6]$) used as internal standard and ground to a fine powder. Absorbance was measured on a Bruker Tensor 27 Fourier transform infrared spectrometer (FT-IR) with a Pike Technology Diffus IR measurement cell. For each sample, 200 spectra were measured from 4000 cm^{-1} to 600 cm^{-1} with a resolution of 4 cm^{-1}, averaged and normalized to the maximum of the C=N stretching vibration at 2118 cm^{-1} of the internal standard.

Variation of Ca/P ratio (Figure S2)

For a facile synthesis of octacalcium phosphate (OCP) with DNA, 30 ng of DNA (synthetic or genomic) was precipitated with disodium phosphate and calcium acetate with a Ca/P ratio of 1.33

To obtain DNA in hydroxyapatite (HAp), ammonium dihydrogen phosphate and calcium acetate were precipitated in a Ca/P ratio of 1.67.

Supplementary Results

Degradation depending on weight loading of DNA in CaP

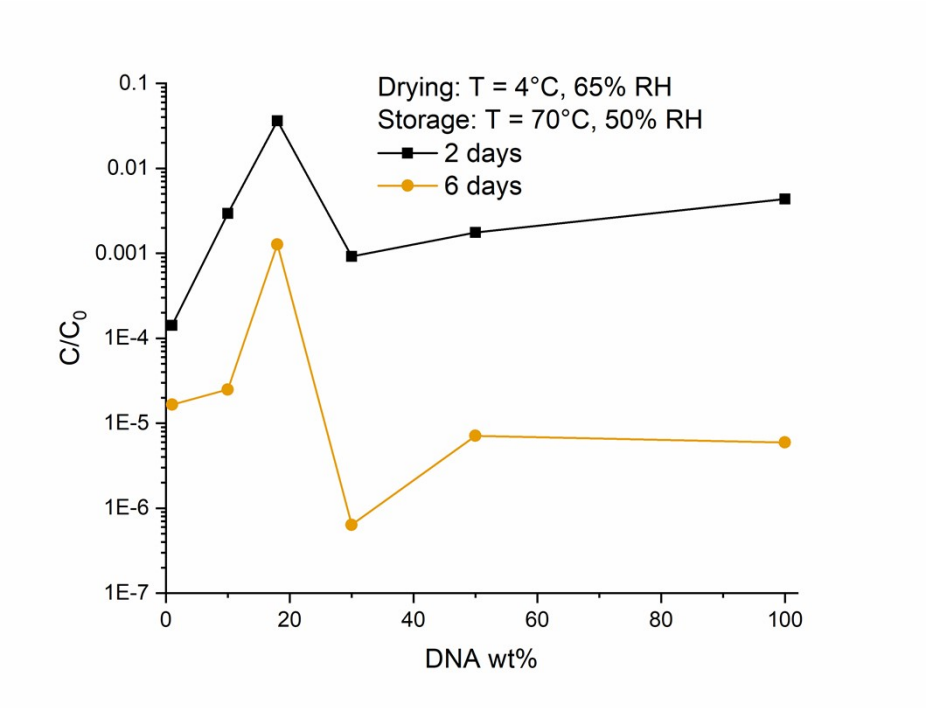

Figure S1: Relative concentration of synthetic DNA after 2 and 6 days at 70°C, 50% RH depending on the DNA weight loading. As previously studied in detail[4] the degradation of DNA is influenced by the total weight load. As a result, 18 wt% was selected as the optimal loading.

Initial accelerated aging experiments

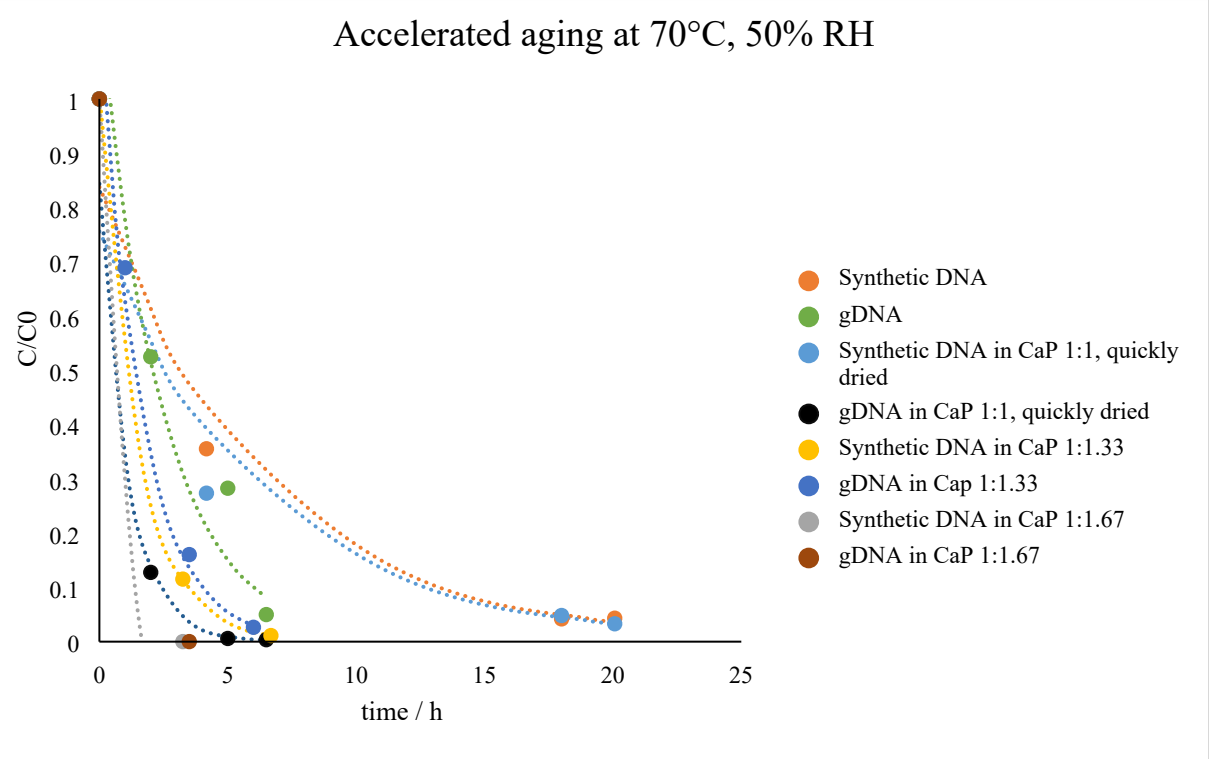

Figure S2: Screening of ideal calcium to phosphate ratio: Accelerated aging decay curves with genomic DNA (gDNA) and synthetic DNA in calcium phosphates of various Ca/P ratios, equivalent to the ratio found in brushite, octacalcium phosphate and hydroxyapatite. All samples were dried at 45°C under vacuum and aging conditions were 70°C, 50% RH. Dotted lines are a guide for the eye. Due to the low stability, no phase identification of Ca/P = 1.33 and Ca/P = 1.67 performed. Ca/P = 1 was further investigated in this study.

SEM: Slowly dried synthetic DNA

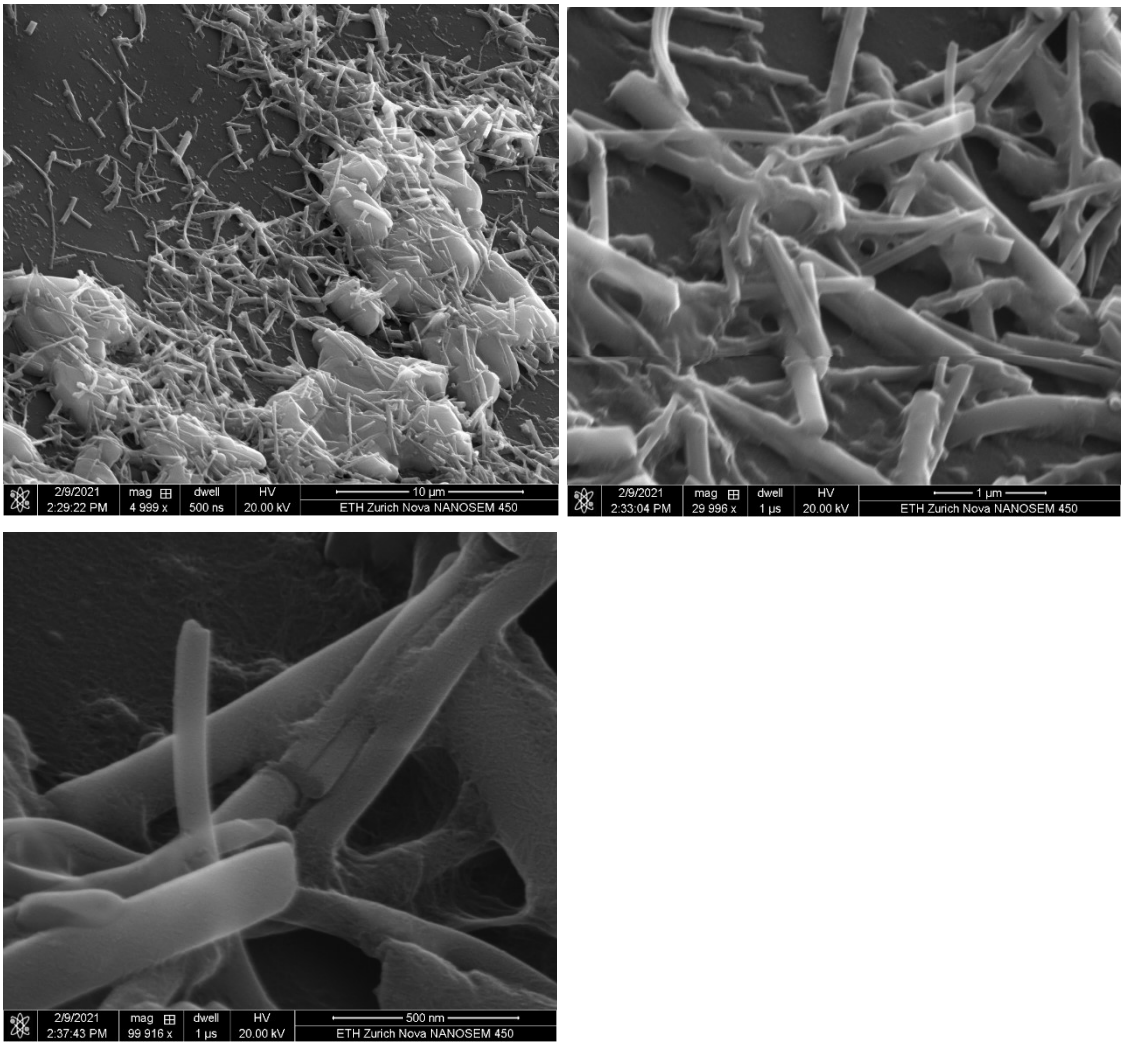

Figure S3: SEM micrographs of slowly dried, synthetic DNA in CaP showing brushite needle-shapes recorded with differing resolutions. Cubic structures belong to sylvite (KCl).

SEM: Slowly dried genomic DNA

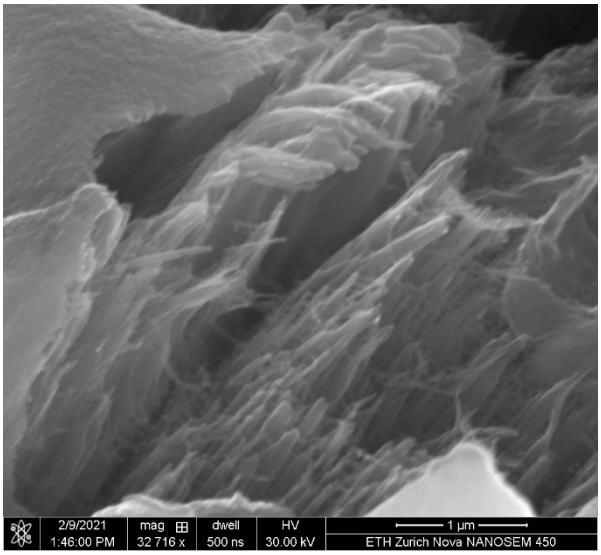

Figure S4: SEM micrograph of slowly dried, genomic DNA in CaP.

SEM: Quickly dried synthetic DNA

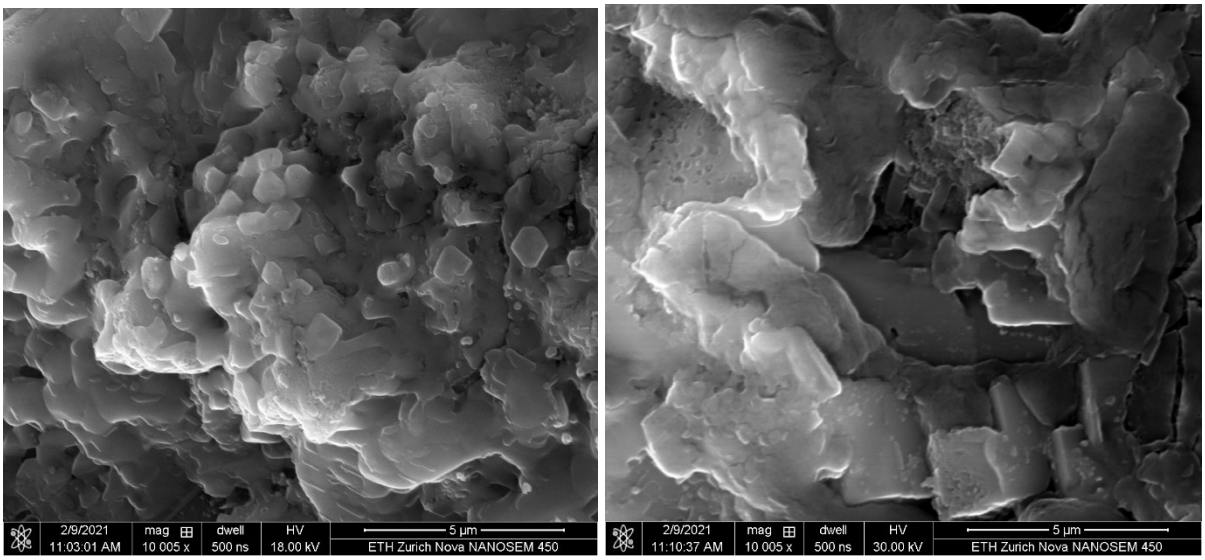

Figure S5: SEM micrographs of quickly dried, synthetic DNA in CaP.

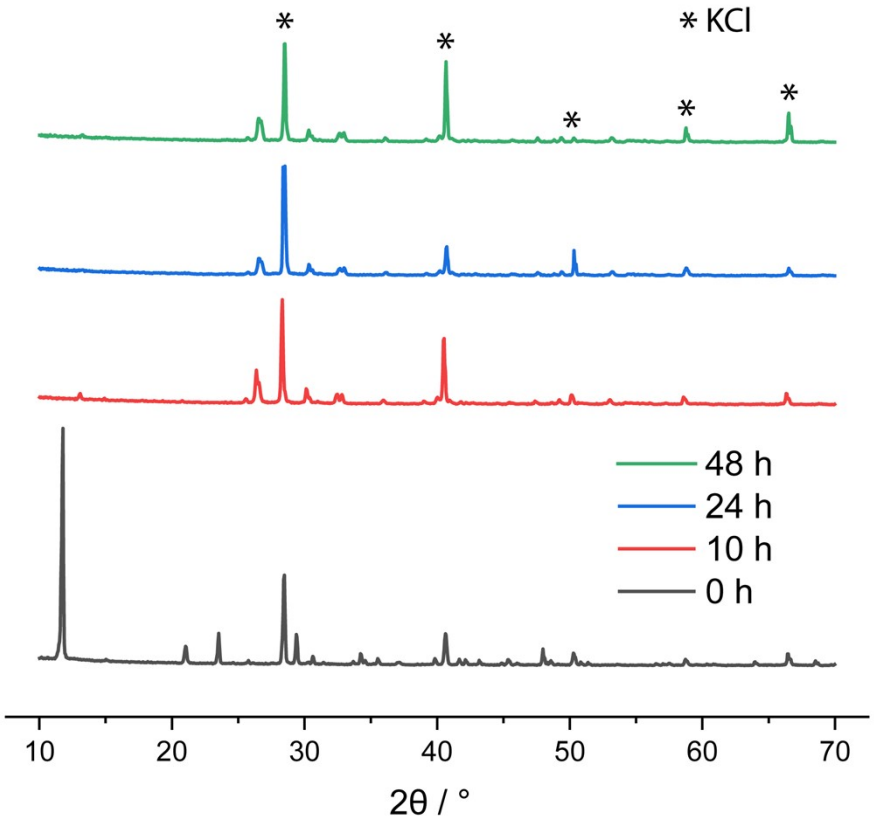

Figure S6: PXRD patterns for DNA in CaP, slowly dried, after indicated times at 70°C and 50% RH. No background correction or normalization.

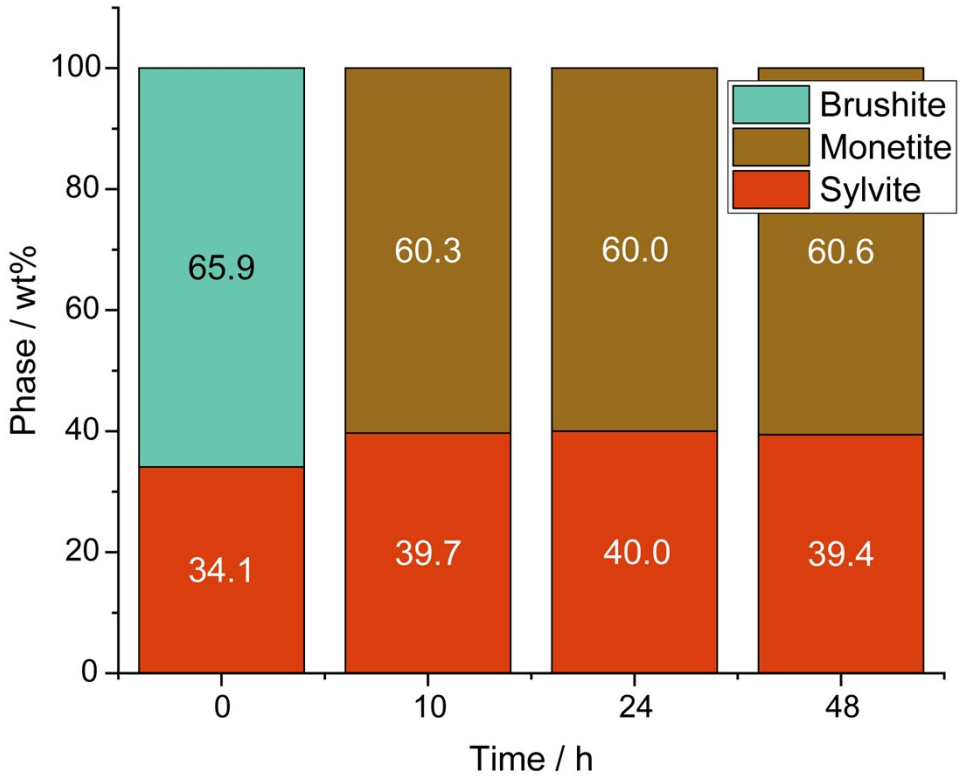

Figure S7: Relative amount of phases present in the slowly dried DNA in CaP quantified from Rietveld analysis (Figure S6). Dicalcium phosphate dihydrate (brushite), dicalcium phosphate (monetite) and potassium chloride (KCl) are the only phases present. Essentially all calcium phosphate present in the sample at t=0h in the form of brushite, transformed to monetite. The slight shift in relative amounts of phases can be explained by the loss of lattice water (brushite to monetite).

Additional PXRD data

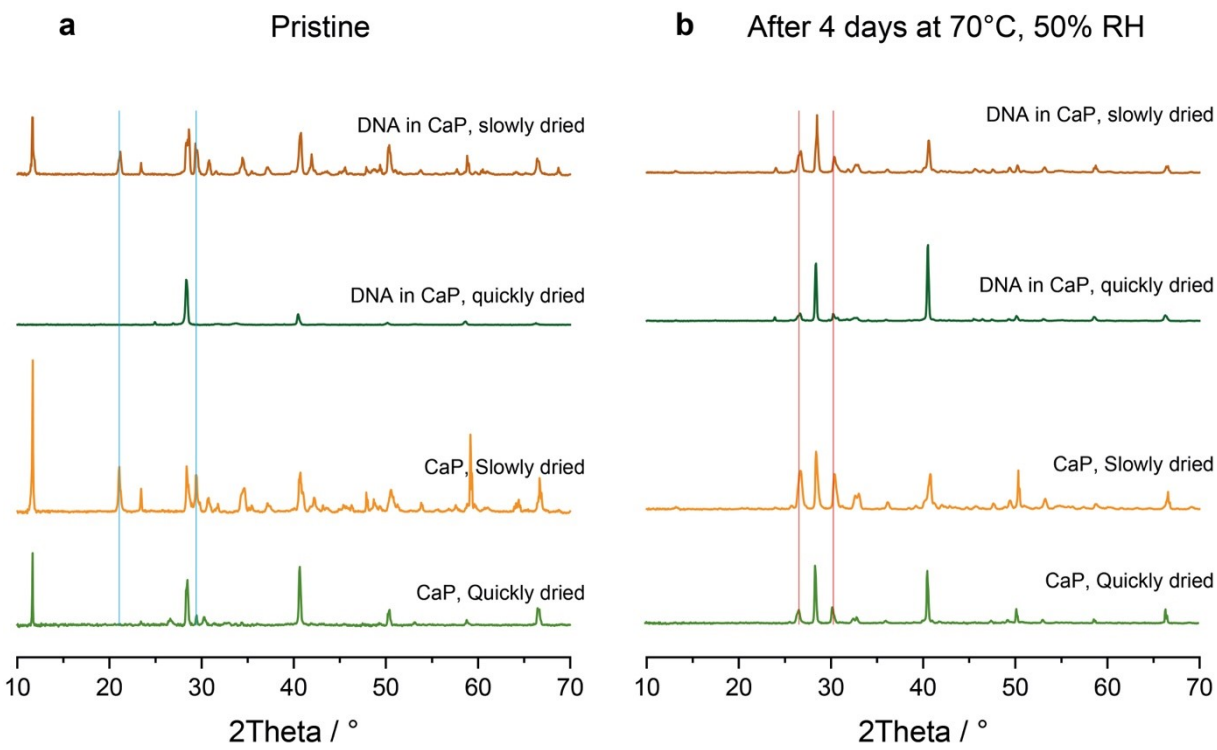

Figure S8: **a** PXRD patterns of CaP and DNA in CaP for slow and quick drying procedures after synthesis. **b** PXRD patterns of CaP and DNA in CaP for slow and quick drying procedures 4 days of accelerated aging conditions (70°C, 50% RH). Most prominent brushite peaks indicated in light blue left, and most prominent monetite peaks indicated in red right (see Fig. 2). The comparison shows that upon precipitation more crystalline brushite structures are formed via slow drying. This is the case for samples with and without DNA. However for the quickly dried sample comprising DNA, no crystalline features other than the sylvite byproduct (KCl) can be observed (see also Fig. 2 in main manuscript). Upon aging, all samples show distinct monetite features, which are most prominent in slowly dried samples. For **a** and **b**, spectra are scaled so that the main peak common byproduct sylvite has an equivalent intensity at 28°.

DRIFTS measurements

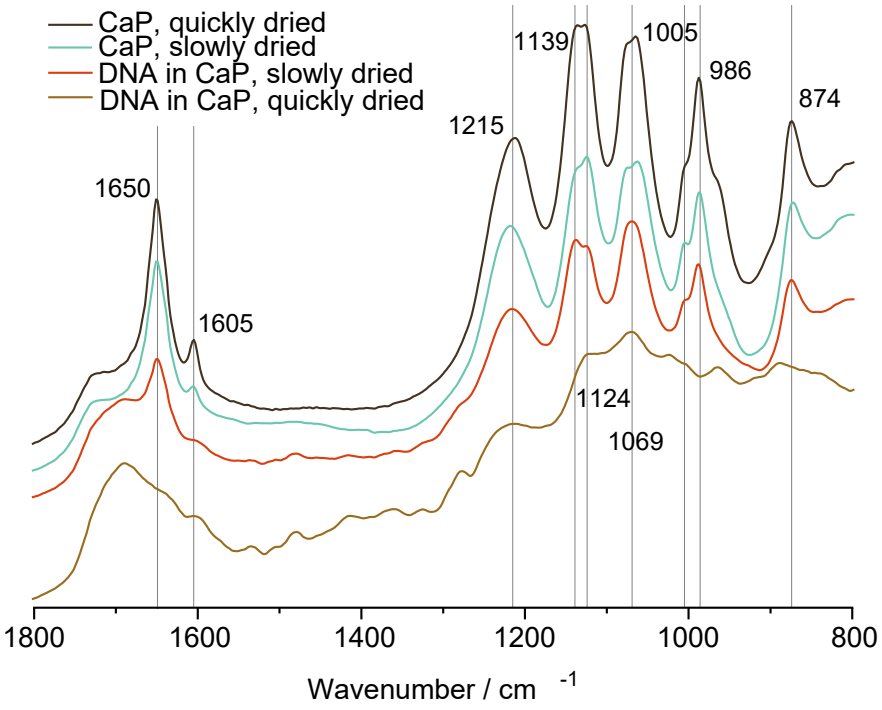

Figure S9 Stacked DRIFTS spectra of slowly and quickly dried CaP with and without DNA. Grey lines with indicated wavenumbers are a guide for the eye. Slowly dried DNA in CaP and CaP without DNA show comparable absorption for water (1600 cm^{-1}) and phosphate (1300 cm^{-1} to 1800 cm^{-1} species, whereas quickly dried DNA in CaP has a very different line shape.

Table S3: Assignments for IR vibrations displayed in Figure 5 in the main text.

Band [cm^{-1}]	Assignment
1650	H-O st
1605	H-O st
1215	H-P-O bend
1139	P-O st
1124	P-O st
1069	P-O st
1005	P-O st
986	P-O st
874	P-O st

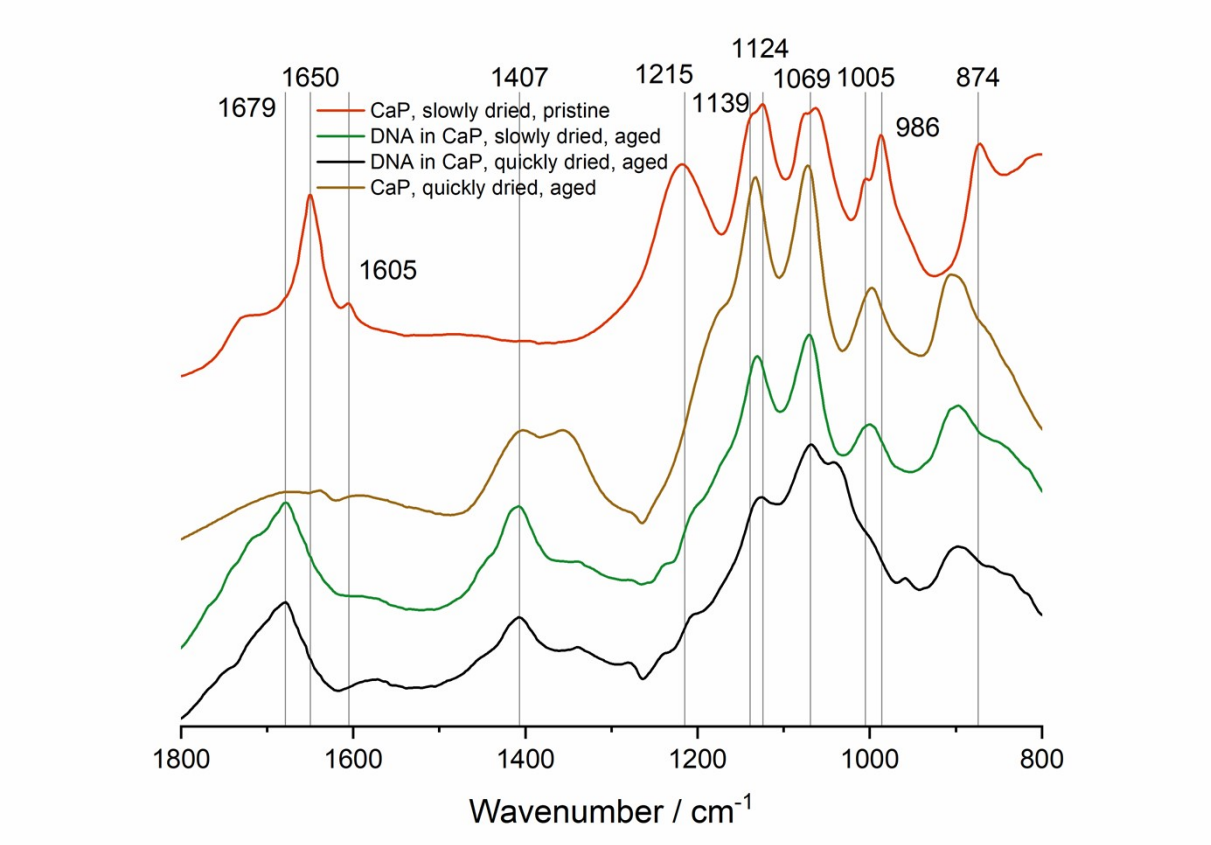

Figure S10: Stacked DRIFTS spectra for CaP and DNA in CaP samples aged for 4 days at 70°C, 50% RH. The spectra underline the findings from PXRD, showing crystalline monetite after 4 days of heat treatment[8]. The absorption at 1679 cm^{-1} visible in both DNA in CaP samples, originates from residual free water O-H bending modes[8] that interestingly do not show in CaP without DNA. P-O-H in plane bending causes absorption around 1400 cm^{-1} which is considerably shifted in comparison to 1215 cm^{-1} in brushite[8] (red curve). An additional red-shifted signal in the same region distinguishes CaP containing DNA from pure CaP. In the range of P-O vibrations between 1200 cm^{-1} and 800 cm^{-1} all spectra are comparable with minor shifts and intensity differences compared to brushite.

Additional EDX element maps

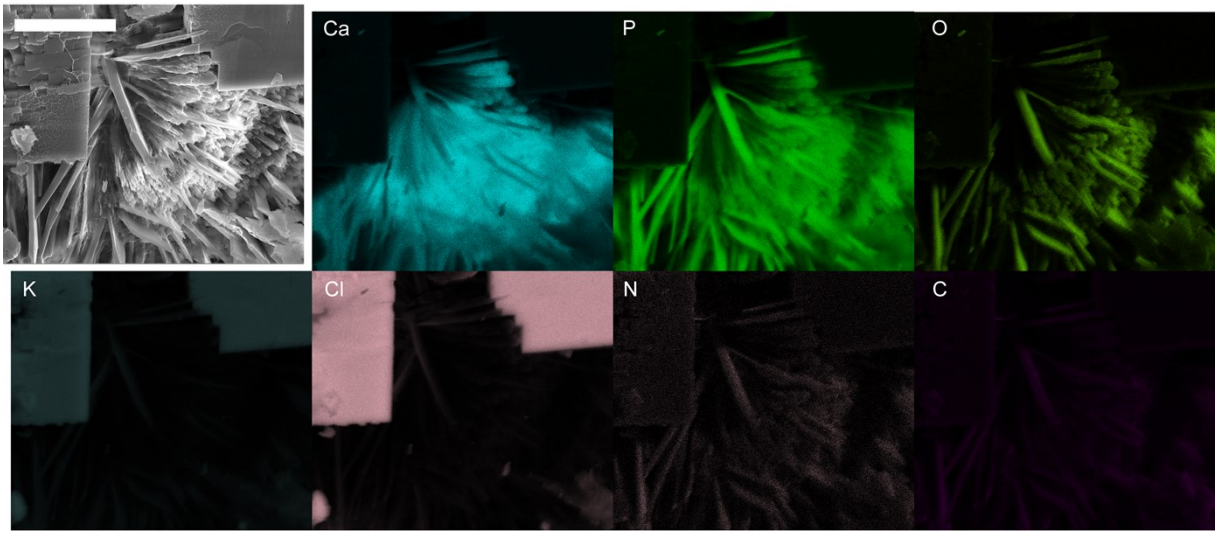

Figure S11: Unaltered, additional EDX element maps for calcium (Ca), phosphorus (P), oxygen (O), potassium (K), chlorine (Cl), nitrogen (N) and carbon (C) atoms. the cubic structures visible in the top left and right corners of the SEM micrograph belong to crystalline potassium chloride (sylvite).

References

1 D. Walker, P. K. Verma, L. M. D. Cranswick, R. L. Jones, S. M. Clark and S. Buhre, *Am. Mineral.*, 2004, **89**, 204–210.

2 P. F. Schofield, K. S. Knight, J. A. M. van der Houwen and E. Valsami-Jones, *Phys. Chem. Miner.*, 2004, **31**, 606–624.

3 A. A. Coelho and IUCr, *urn:issn:1600-5767*, 2018, **51**, 210–218.

4 A. X. Kohll, P. L. Antkowiak, W. D. Chen, B. H. Nguyen, W. J. Stark, L. Ceze, K. Strauss and R. N. Grass, *Chem. Commun.*, 2020, **56**, 3613–3616.

5 Y. Minegishi, M. K.-S. Wong, T. Kanbe, H. Araki, T. Kashiwabara, M. Ijichi, K. Kogure and S. Hyodo, *PLoS One*, 2019, **14**, e0222052.

6 Z. Xiang-bo, W. Zhi-ping, D. Jian-min, L. Jian-zhong and M. Bao-liang, *BMC Urol.*, 2005, **5**, 1–6.

7 Y. Han, L. Han, Y. Yao, Y. Li and X. Liu, *Anal. Methods*, 2018, **10**, 2436–2443.

8 L. Tortet, J. R. Gavarri, G. Nihoul and A. J. Dianoux, *J. Solid State Chem.*, 1997, **132**, 6–16.

9 L. Orlando, A. Ginolhac, G. Zhang, D. Froese, A. Albrechtsen, M. Stiller, M. Schubert, E. Cappellini, B. Petersen, I. Moltke, P. L. F. Johnson, M. Fumagalli, J. T. Vilstrup, M. Raghavan, T. Korneliussen, A. S. Malaspinas, J. Vogt, D. Szklarczyk, C. D. Kelstrup, J. Vinther, A. Dolocan, J. Stenderup, A. M. V Velazquez, J. Cahill, M. Rasmussen, X. Wang, J. Min, G. D. Zazula, A. Seguin-Orlando, C. Mortensen, K. Magnussen, J. F. Thompson, J. Weinstock, K. Gregersen, K. H. Røed, V. Eisenmann, C. J. Rubin, D. C. Miller, D. F. Antczak, M. F. Bertelsen, S. Brunak, K. A. S. Al-Rasheid, O. Ryder, L. Andersson, J. Mundy, A. Krogh, M. T. P. Gilbert, K. Kjær, T. Sicheritz-Ponten, L. J. Jensen, J. V Olsen, M. Hofreiter, R. Nielsen, B. Shapiro, J. Wang and E. Willerslev, *Nature*, 2013, **499**, 74–78.

10 T. van der Valk, P. Pečnerová, D. Díez-del-Molino, A. Bergström, J. Oppenheimer, S. Hartmann, G. Xenikoudakis, J. A. Thomas, M. Dehasque, E. Sağlıcan, F. R. Fidan, I. Barnes, S. Liu, M. Somel, P. D. Heintzman, P. Nikolskiy, B. Shapiro, P. Skoglund, M. Hofreiter, A. M. Lister, A. Götherström and L. Dalén, *Nature*, 2021, **591**, 265–269.

11 H. B. Hansen, P. B. Damgaard, A. Margaryan, J. Stenderup, N. Lynnerup, E. Willerslev and M. E. Allentoft, *PLoS One*, 2017, **12**, 1–18.

12 L. Schröter, F. Kaiser, S. Stein, U. Gbureck and A. Ignatius, *Acta Biomater.*, 2020, 117, 1–20.

13 B. R. Constantz, B. M. Barr, I. C. Ison, M. T. Fulmer, J. Baker, L. A. McKinney, S. B. Goodman, S. Gunasekaren, D. C. Delaney, J. Ross and R. D. Poser, *J. Biomed. Mater. Res.*, 1998, **43**, 451–461.

14 P. Frayssinet, L. Gineste, P. Conte, J. Fages and N. Rouquet, *Biomaterials*, 1998, **19**, 971–977.

15 M. Sadat-Shojai, M. T. Khorasani, E. Dinpanah-Khoshdargi and A. Jamshidi, *Acta Biomater.*, 2013, **9**, 7591–7621.

16 S. V Dorozhkin, *Biomatter*, 2011, **1**, 121–164.

17 K. Ioku, G. Kawachi, S. Sasaki, H. Fujimori and S. Goto, *J. Mater. Sci.*, 2006, **41**, 1341–1344.

18 H. Zhang and B. W. Darvell, *Acta Biomater.*, 2011, **7**, 2960–2968.

19 R. Z. LeGeros and J. P. LeGeros, in *An Introduction to Bioceramics*, World Scientific, 1993, pp. 139–180.

20 M. Okazaki, Y. Yoshida, S. Yamaguchi, M. Kaneno and J. C. Elliott, *Biomaterials*, 2001, **22**, 2459–2464.

21 N. Nassif, F. Martineau, O. Syzgantseva, F. Gobeaux, M. Willinger, T. Coradin, S. Cassaignon, T. Azaïs and M. M. Giraud-Guille, *Chem. Mater.*, 2010, **22**, 3653–3663.